*Journal of Thermal Analysis, Vol. 47 (1996) 1013-1026*

# MODULATED DIFFERENTIAL SCANNING CALORIMETRY IN THE GLASS TRANSITION REGION II. The mathematical treatment of the kinetics of the glass transition*

*B. Wunderlich, A. Boller, I. Okazaki** and S. Kreitmeier****

Department of Chemistry, The University of Tennessee, Knoxville, TN 37996-1600, and Chemistry and Analytical Sciences Division, Oak Ridge National Laboratory, Oak Ridge TN 37831-6197, USA

## Abstract

Temperature-modulated differential scanning calorimetry (TMDSC) is based on heat flow and represents a linear system for the measurement of heat capacity. As long as the measurements are carried out close to steady state and only a negligible temperature gradient exists within the sample, quantitative data can be gathered as a function of modulation frequency. Applied to the glass transition, such measurements permit the determination the kinetic parameters of the material. Based on either the hole theory of liquids or irreversible thermodynamics, the necessary equations are derived to describe the apparent heat capacity as a function of frequency.

**Keywords:** activation energy, calorimetry, glass transition, heat capacity, heat flow calorimeter, hole theory, irreversible thermodynamics, TMDSC, modulated calorimetry

## Introduction

Modulated differential scanning calorimetry, MDSC, [1] is based on temperature modulation and has recently also been called TMDSC [2]. The mathematical treatment described in this paper uses the formalism developed for heat-flux calorimetry, as can be carried out with the TA Instruments MDSC 2920, and is based on the prior, standard analysis of the glass transition by dynamic differential thermal analysis, DDTA, that was first used in 1963 [3]. Data obtained with alternating differential scanning calorimetry (ADSC, Mettler-Toledo) or dynamic differential scanning calorimetry, (DDSC, Perkin-Elmer)

* Presented in part at the 24th Conference of the Northamerican Thermal Analysis Society, San Francisco, CA, September 10–13, 1995.

** On leave from Toray Industries, Inc., Otsu, Shiga 520, Japan.

*** Present address: University at Regensburg, Polymerphysik, Regensburg, D-93040, Germany.

*0368–4466/96/ $ 5.00*

*John Wiley & Sons, Limited*
*Chichester*

can be treated similarly after it is established that the system used is linear and the modulation does not introduce undue lags.

In prior publications from our laboratory we have given a general mathematical description of MDSC [4], discussed a method of quasi-isothermal MDSC and gave the necessary calibration instructions and limits for producing high-quality data [5], and also addressed the questions of linearity, steady state, and complex heat capacity [6]. In the first paper of this series on the MDSC of the glass transition region, a qualitative study of polystyrene was given, showing the separation of the frequency effect of the modulation and the time effect of the underlying heating rate [7]. A quantitative evaluation of experimental data on polystyrene and poly(ethylene terephthalate) based on the present paper will be published as part III in this series [8]. A general, computer-generated lecture course on MDSC was produced, and is available through the World Wide Web [9].

## The glass transition

The glass transition is the major time-dependent transition in condensed matter [10]. It separates corresponding solid and mobile states of the same amount of disorder. In solids, small-amplitude vibrations with a fixed, average position and a time scale of picoseconds ($10^{-12}$ s) or less are the dominant thermal motion. In the mobile states, additional large-amplitude motion, such as translation, rotation, and internal rotation (conformational motion) cause the typical macroscopic mobility. Although the molecular time scale for large-amplitude motion is also in the picosecond range, macroscopic effects may be slow due to the needed cooperativity of many elementary steps. The mechanisms of thermal motion and defect formation in crystals have been studied using molecular dynamics simulations of systems with up to 30000 atoms [11].

The mobile states of matter can be divided into melts, liquid crystals, plastic crystals, and conformationally disordered crystals (condis crystals) [12]. These mobile phases are linked to their corresponding glasses (solids) through glass transitions. Each fully mobile part of the molecule (bead) contributes an approximately fixed quantity to the heat capacity at the glass transition [13]. The basic glass transition of liquids is known for many years [14]. It is seen on vitrification of liquids that are unable to crystallize for kinetic or structural reasons. The problems of assignment of the glass transition were recently reviewed in a symposium of the American Society for Testing of Materials (ASTM) [15]. An operational definition of the glass transition temperature, $T_g$, fixes it at the point of half-vitrification or devitrification as indicated, for example, by the temperature where half the increase or decrease of heat capacity, $\Delta C_p$, is reached [16]. Naturally this point is time dependent. Special problems arise for the glass transitions in partially ordered systems [17]. It will also be of

interest to extend the kinetic analysis developed in this paper in the future to the glass transitions in partially ordered systems that show several unexplained effects, such as a broadened glass transition range, a rigid amorphous fraction, and occasionally a loss of enthalpy relaxation.

In the present discussion, the hole theory of the liquid state is used as a simple model that can explain a glass transition-like behavior. Other models can be treated similarly. Especially the kinetics of the approach to equilibrium as given by irreversible thermodynamics can easily be adapted to the derived equations [10]. The hole theory was developed in the 1930s by Frenkel and Eyring [18]. It uses only a minimum of parameters. One assumes, that a liquid in equilibrium has a number of holes, $N^*$ that depends on temperature. The energy required to produce a hole, the hole energy, is $\varepsilon_h$, and can be estimated from the difference in heat capacity between liquid and solid, and the known cohesive energy density [13]. The heat capacities of many liquid and solid polymers are available in the ATHAS Data Bank [19]. The kinetics of the hole formation is, furthermore, governed by an activation energy, $\varepsilon_j$, and a preexponential factor, $B$, that contains the partition function ratio of the involved configurations during hole formation [3]. At the glass transition, the hole-equilibrium freezes because not enough time is available to establish the hole equilibrium. The application of the hole theory to the glass transition was first suggested by Hirai and Eyring [20] and applied shortly thereafter to calorimetry, using DDTA [3].

## Modulated calorimetry and steady state

In MDSC a simple, sinusoidal modulation changes the block temperature $T_b(t)$ to:

$$T_b(t) = T_o + <q>t + A_{T_b} \sin(\omega t)) \tag{1}$$

where $<q>$ is the underlying heating rate, obtained by averaging over a fixed number of complete modulation periods; $\omega$, the modulation frequency $2\pi/p$, with $p$ representing the period of one cycle in seconds. The amplitude $A_{Tb}$ is adjusted such that a preset amplitude $A$ is observed at the sample position. Typical modulations may have an amplitude $A$ of 0.5 to 2 K and a period of 10 to 100 s. The condition for quantitative measurement must maintain a negligible temperature gradient within the sample [5, 6, 10]. Actual run parameters were established earlier [5].

The change in temperature as a function of time at the sample position of the calorimeter is given by [4]:

$$T_s(t) - T_o - <qt> = -q\frac{C_s}{K}\left(1 - e^{-K\iota/C_s}\right) + \\ + A[\cos\varepsilon \sin\omega t - \sin\varepsilon \cos\omega t + \sin\varepsilon\, e^{-K\iota/C_s}] \tag{2}$$

where $T_s(t)$ is the time-dependent sample temperature; $T_o$, the temperature at the start of the experiment; $C_s$, the heat capacity of the sample calorimeter; $K$, the Newton's law constant; and $\varepsilon$, the phase shift relative to the block temperature:

$$\sin\varepsilon = \frac{\omega}{\sqrt{(K/C_s)^2 + \omega^2}} \tag{3}$$

The relationship $\cos\varepsilon \sin\omega t - \sin\varepsilon \cos\omega t = \sin(\omega t - \varepsilon)$ can condense Eq. (2) and the equation $\sin^2\varepsilon + \cos^2\varepsilon = 1$ permits evaluation of $\cos\varepsilon$. Steady state is reached in the presence of modulation as soon as $e^{-Kt/C_s}$ becomes negligible. Analogous equations hold for the reference temperature and the temperature difference (equivalent to heat flow *HF*) with phase shifts of $\varphi$ and $\delta$, respectively. The calibration of $K$ and measurement of $A_\Delta$, the modulation amplitude of the temperature difference (or heat flow *HF*), allows then the calculation of the heat capacity at a given $A$ and $\omega$:

$$mc_p = \frac{A_\Delta}{A}\sqrt{(K/\omega)^2 + C'^2} = \frac{A_\Delta}{A} \times K' \tag{4}$$

where $m$ is the sample mass; $c_p$, the specific heat capacity; $C'$, the heat capacity of the empty reference calorimeter of identical mass to the empty sample calorimeter. The calibration constant $K$ is independent of modulation frequency and reference heat capacity, $K'$ changes on changing $\omega$ and $C'$.

Specially important is a knowledge of the change of steady state as one goes through heat capacity changes as, for example, in the glass transition coupled with a hysteresis peak, or a broad melting peak with a possibility of exothermic crystal perfection. To get a more quantitative insight into the distance from steady state, the calorimeter with the larger heat capacity (sample calorimeter) is analyzed. If it reaches a given percentage deviation from steady state, set for the present discussion at 5%, steady state is considered to be lost. The somewhat large error is chosen since for the heat flow *HF* (or $\Delta T$), both, the reference temperature $T_r$ and $T_s$ deviate from steady state and the difference should show a somewhat smaller error. Also, all calculations are carried out with a value of 50 s for $C_s/K$, a value on the large side for present day DSC. Typical values for $C_s/K$ may range from 1–100 s, depending on instrument construction and $C_s$, the sample plus pan heat capacity. The modulation amplitude $A$ is taken to be 1.0 K, and the underlying heating rate $<q> = 3.0$ K min$^{-1}$ (0.05 K s$^{-1}$). Equation (2) can then be rewritten to express the distance from steady state $\Lambda$ (in K):

$$\Lambda = T_s(t) - T_o - <q>t + q\frac{C_s}{K} - A[\sin(\omega t - \varepsilon)] = \left[q\frac{C_s}{K} + A\sin\varepsilon\right] e^{-Kt/C_s} \tag{5}$$

With the parameters just given, $\Lambda \approx 3 \exp(-t/50)$, and it takes about 200 seconds to reach the 5% value when starting the measurement from $T_b = T_s = T_r = T_o$ (begin

of the experiment, $t=0$). The approximate steady-state lag of the temperature due to the underlying heating rate is $<q>C_s/K=2.5$ K, i.e. it is the dominating effect under the given conditions. For large modulation amplitudes and small values of $C_s/K$ and/or $<q>$ the second term of Eq. (5) may well be more important.

Any subsequent change in $C_s$ will cause a new deviation from steady state that can be estimated analogously because of the linearity of the heat flux equation [6]. An instantaneous, stepwise increase in heat capacity causes a deviation from steady state $\Lambda$ that dies off with the exponential given by Eq. (5) (note that $C_s$ enters also into $\varepsilon$).

For a severe test of the lag during a glass transition, data for (hypothetical) amorphous polyethylene are used. The increase in $C_p$ is 10 J (K mol)$^{-1}$ at the glass transition temperature, $T_g$ at 237 K, and the heat capacity of the solid is about 20 J (K mol)$^{-1}$. Assuming, furthermore, the glass transition occurs linearly over a temperature range of about 10 K (5% increase in heat capacity per kelvin of temperature increase), the plot of the lags is given in Fig. 1 by adding the appropriate multiple terms derived from Eq. (5). The filled squares represent the increase in heat capacity in a lag-free experiment. The computed $T_s$ shows the sample temperature one should be able to observe. The difference is the lag. The lag of 3 K in fixing the glass transition temperature shown in the figure is, perhaps, still acceptable for common determinations of the glass transition, but must be corrected for in discussing the kinetics of the glass transition. The deviation of the heat capacity by more than 10% between 235 and 243 K is certainly not acceptable as a quantitative result. For the reporting of $C_p$ for the ATHAS Data Bank [19] this error was in the past eliminated by extrapolation of the solid and liquid heat capacities to $T_g$. For integration of the

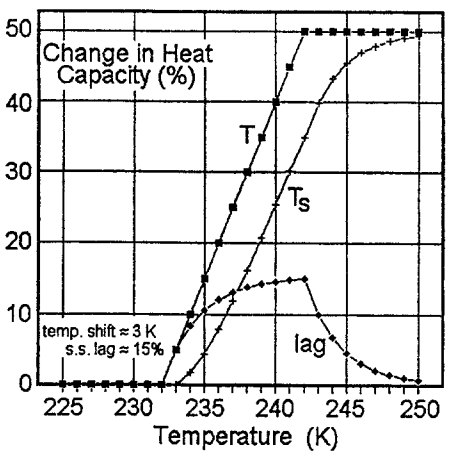


**Fig. 1** Lags in the glass transition region. The curve labelled $T$ is the lag-free temperature (assumed); $T_s$, the sample temperature with lag; lag, the error in heat capacity under the chosen (extreme) conditions, see text

heat capacities to enthalpy, it was then assumed that a vertical increase of $\Delta C_p$ occurs at $T_g$. Comparing the polyethylene case with polystyrene or poly(ethylene terephthalate), two polymers that are often used as standards [8], one sees changes of heat capacity of 19 and 30% at the glass transition, i.e. their lags are closer to the 5% error in heat capacity. Similarly, a reduction of $C_s$ and $\varepsilon$ enables quantitative heat capacity measurements through the glass transition by staying close to steady state. For highest precision, two sets of measurement should be made. One with large $C_s$ for the measurement of solid and liquid heat capacities, and one with small $C_s$ in the glass transition region for the study of the kinetics. The latter is discussed next.

## The kinetics of the glass transition

A qualitative analysis of the superposition of the reversible and irreversible processes in the glass transition region is schematically illustrated in Fig. 2. Somewhat below the glass transition temperature, $T_g$, the heat capacity consists practically only of vibrational contributions. Molecular dynamics simulations have shown that steady state for the vibrations in solids can be reached in picoseconds [11]. This time scale is practically instantaneous, and one can represent the solid heat capacity simply by its vibrational, time-independent contribution $C_{p_o}$:

$$C_p \text{ (solid)} = C_{p_o} \tag{6}$$

The vibrational heat capacity $C_{p_o}$ is available through the Advanced THermal Analysis System, ATHAS [19]. The parallel thin lines in the figure represent the enthalpies $H(=\int C_p dT)$ of various glasses cooled at different rates (higher cooling rates for larger values of $H$). Once in the glassy state, all heat capacities (slopes of $H$) are closely similar but, as shown, not the enthalpies.

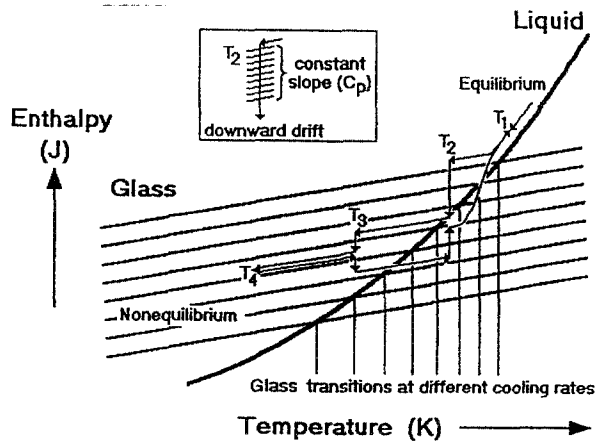


**Fig. 2** Schematic of the enthalpy in the glass transition region [5, 7]

In the liquid state, longer times are necessary to reach thermal equilibrium because of the need of the molecules to undergo the larger, cooperative, structural changes. The hole equilibrium models the additional contribution to the heat capacity. It is given by the change in number of holes with temperature under equilibrium conditions:

$$C_p(\text{liquid}) = C_{p_o} + \varepsilon_h\left(\frac{dN^*}{dT}\right) \tag{7}$$

In the later discussion, the change in equilibrium number of holes with temperature, $dN^*/dT$ will be set equal to $\alpha$. Creation, motion, and destructions of holes are cooperative kinetic processes and may be slow. This leads to deviations from Eq. (7) if the measurement is carried out faster than the kinetics of the hole equilibrium allows. Applied to the glass transition, one can write a simple, first-order kinetics expression to describe the time-dependence of the actual number of holes in the glass-transition region:

$$\left(\frac{dN}{dt}\right) = \frac{1}{\tau}(N^* - N) \tag{8}$$

In Eq. (8) $N$ represents the instantaneous number of holes, $N^*$, the equilibrium number of holes, and $\tau$ is the relaxation time for the formation of holes. For both $N^*$ and $\tau$ more detailed expressions are available through the hole theory [3]. In case one wants to describe the glass transition with irreversible thermodynamics to be independent of a specific model, the same equation can be used. The number of holes is then replaced by $\zeta$, the appropriate internal variable, and $1/\tau$ is proportional to the curvature of the free energy relative to the relaxing internal variable at equilibrium. The proportionality constant is the so-called phenomenological coefficient [10]. Equation (8) holds always close to equilibrium. The better the kinetics is modeled by Eq. (8), the further from equilibrium can it be used.

Some five to ten kelvins above $T_g$, most one-phase and one-component systems show no kinetic effects for typical DSC heating or cooling rates (1–20 K $min^{-1}$). The heat capacity is then equal to the slope of the heavy curve in Fig. 2. On going through $T_g$, the glassy state is reached at different temperatures for different cooling rates. Each cooling rate corresponds to freezing a different number of holes, giving rise to the multitude of glasses with distinct enthalpies, as indicated in the figure. In the temperature range where modulation frequency or underlying heating rate and relaxation times are comparable, Eq. (8) must be considered.

A detailed MDSC analysis involves step-wise cooling and heating with long-time quasi-isothermal measurements. Let us consider steps between $T_1$ and $T_4$ [5, 7]. In such experiment $<q>$ is zero and the effect of modulation frequency

is easily assessed. The case of linear heating rate without modulation was treated before [3]. At $T_1$ the sample remains in equilibrium and the heat capacity is represented by Eq. (7). The effect of the kinetics can be included in Eq. (7) by writing:

$$C_p^{\#}(\text{liquid}) - C_{p_o} = \varepsilon_h\left[\left(\frac{\partial N}{\partial T}\right)_t + \left(\frac{\partial N}{\partial t}\right)_T\left(\frac{dt}{dT}\right)\right] \tag{9}$$

In this quasi-isothermal experiment $dt/dT$ is fixed by the modulation as $1/(\omega \cos\omega t)$ and $\partial N/\partial T$ is small. The time dependent contribution of the holes to $C_p$, the apparent $\Delta C_p^{\#}$, is (using $\sec\theta = 1/\cos\theta$):

$$C_p^{\#}(\text{liquid}) - C_{p_o} = \Delta C_p^{\#} = \frac{\varepsilon_h \sec \omega t}{A\omega}\left(\frac{dN}{dt}\right) \tag{10}$$

where the modulation frequency $\omega$ is chosen to refer to the liquid sample [$=\omega t - \varepsilon$ of Eqs (2) and (5)]. In case of short relaxation times, equilibrium is reached without delay and the change in number of holes, $dN/dt = A\alpha\omega \cos\omega t$, so that $\Delta C_p = \varepsilon_h \alpha$, as expected from Eq. (7).

Cooling quickly to $T_2$ yields initially a glass, represented by the upper thin enthalpy line. At this temperature the modulation frequency is already too fast to measure anything but the heat capacity of the glass given by $C_{p_o}$. Since the measurement is carried out over many modulation cycles, the enthalpy relaxes slowly in an irreversible process to the lower levels of enthalpy (as indicated by the vertical arrow). The rate of these enthalpy changes are little affected by the small temperature modulation, and thus not measured as a reversing contribution by MDSC ($N^*$ and $\tau$ can be assumed to be independent of modulation at this temperature). In a measurement with an appropriate heating rate $<q>$, the change in enthalpy appears in the nonreversing part of the heat flow as a typical hysteresis peak (enthalpy relaxation) [7]. The result can be expressed as:

$$\Delta H(t) = \varepsilon_h(N^* - N_o)e^{-(t-t_o)/\tau} \tag{11}$$

with $\Delta H(t)$ representing the enthalpy change between the initial time $t_o$ and $t$. Equation (11) can be derived by multiplication of Eq. (8) with $\varepsilon_h$ and integration from $t_o$ to $t$. The center insert illustrates this downward drift in $H$ at $T_2$. Even if ultimately the equilibrium liquid were reached, as suggested in the figure, the measured heat capacity would still be that of the solid, since the hole equilibrium does not change significantly during a single modulation period. Continuing to $T_3$, the enthalpy relaxation is less because of a larger $\tau$, but again, unrecorded in the reversing heat capacity measurement. At $T_4$, finally, a metastable glass has been reached.

On reheating, the relaxations at $T_3$ and $T_2$ would, again, not be recorded as reversing effect, but note that the direction of the enthalpy relaxation is reversed. After the jump to $T_1$, finally, the relaxation time is sufficiently short so that $C_p$ is represented by Eq. (7). On cooling and heating between $T_1$ and $T_2$ the heat capacity is intermediate between Eqs (6) and (7), giving a glass transition temperature at half-vitrification that is governed by the time scale of modulation.

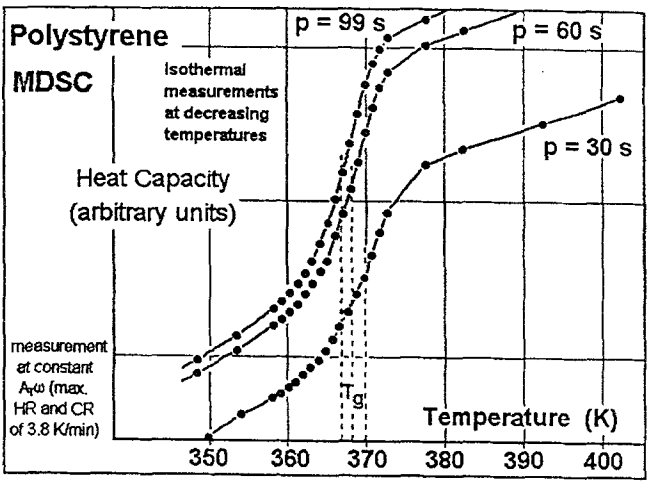


**Fig. 3** Data of the heat capacity of polystyrene in the glass transition region measured at different frequency [7]

To follow the kinetics of the glass transition quantitatively in the critical temperature region between $T_1$ and $T_2$, we use quasi-isothermal experimentation with a sufficiently small amount of sample (small $C_s/K$) and modulation to make the lag within the sample during the glass transition acceptable [Fig. 1 and Eq. (5)]. In such experiment the second time scale introduced by the underlying heating rate $<q>$ is eliminated and the mathematical analysis is simplified. Figure 3 shows a set of data for polystyrene [7]. The amplitude of modulation was chosen to give constant maximum heating and cooling rates of 3.8 K $min^{-1}$ for all three series of experiments. Inserting the maximum value for $\varepsilon(A_{T_s} \sin\varepsilon \leq 1)$ into Eq. (5) proves that the heat-flux MDSC can reproduce the change in heat capacity without significant lag due to heat conduction, i.e. one can analyze the observed heat capacity directly with the kinetics of the glass transition as given by Eq. (8).

The solution of Eq. (8) was given before as [3, 21 ]:

$$N(t) = N(t_o)\, e^{-\Phi(t)} + e^{-\Phi(t)} \int_{t_o}^{t} \frac{N^*(t')}{\tau(t')}\, e^{\Phi(t)} dt'$$

$$\Phi(t) = \int_{t_o}^{t} \frac{1}{\tau(t')} dt' \tag{12}$$

where $t_o$ is the beginning of the experiment, and $\Phi(t)$ is the time-averaged (time)/(relaxation time) ratio. Both $\tau$ and $N^*$ are to be inserted into Eq. (12) with their proper temperature and (through the modulation) time dependence.

For the temperature dependence over the small modulation amplitude, one can assume that $\tau$ can change with an Arrhenius temperature dependence [$\tau=B\ \exp\{\varepsilon_j/(RT)\}$]. From the hole-theory a more detailed expression is available [3]. With the modulation $T=T_o+A\ \sin\omega t$, the time-dependence of $\tau$ can be written as:

$$\tau(t') = B\ e^{\varepsilon_j/[RT_o\ (1\ +\ \{A/T_o\}\ \sin\omega t')]} \tag{13}$$

with $T_o$ representing the quasi-isothermal base temperature. This expression leads to a rather involved Eq.(12) that can be solved, but is rather unhandy for comparison with the experiment. One notices, however, that the modulation amplitude $A/T_o$ is quite small, so that it is possible first to replace $[1+(A/T_o)\ \sin\omega t]^{-1}$ by $[1-(A/T_o)\ \sin\omega t]$, and then develop the exponent into a series, keeping only the first two terms ($e^{-x}=1-x+x^2/2-\ldots$), so that:

$$\tau = \tau_o\left(1 - \frac{A\varepsilon_j}{RT_o^2}\ \sin\omega t'\right) \tag{14}$$

with $\tau_o$ representing $\tau$ at $T_o$ [$\tau_o=B\ \exp\{\varepsilon_j/(RT_o)\}$]. Equation (14) can now be integrated to get an expression for $\Phi(t)$:

$$\Phi(t) = \frac{1}{\tau_o}\left[t + \frac{A\varepsilon_j}{RT_o^2\omega}\ (1 - \cos\omega t)\right] \tag{15}$$

During the initial moments of the modulation, the whole expression must be used to assess the hole equilibrium, but very soon, an almost modulation-independent value of $\Phi(t)$ results that is, as in the temperature independent case $= (t-t_o)/\tau$. With this value Eq. (12) can now be solved more easily.

To get an expression that can easily linked to experiment let us first treat the case that $N^*$ is temperature dependent in the modulation range ($dN^*/dT=\alpha$) and $\tau$ is not, i.e. $\tau(t)=\tau_o$. The system will in this case reach a symmetrical steady-state of a reversing number of holes in the sample with a characteristic phase lag of $\gamma$ relative to $\omega t$. The solution of Eq. (8) is under these conditions:

$$N(t) = N_o\ e^{-t/\tau_o} + e^{-t/\tau_o}\int_{t_o}^{t} \frac{N_o^* + A\alpha\ \sin\omega t'}{\tau_o} e^{t/\tau_o}\ dt' \tag{16}$$

with $N_o$ representing the number of holes at the beginning of the experiment. This equation can easily be integrated. Setting to equal to zero, one finds by setting:

$$\gamma = \arcsin \frac{\omega}{\sqrt{(1/\tau_o)^2 + \omega^2}} \tag{17}$$

and:

$$\gamma = \arccos \frac{1/\tau_o}{\sqrt{(1/\tau_o)^2 + \omega^2}} \tag{18}$$

a solution that is similar to the approach to steady state due to heat flow [Eq. (2)]:

$$N - N_o^* = (N_o - N_o^*)e^{-t/\tau_o} + A\alpha \sin\gamma \cos\gamma\, e^{-t/\tau_o} + A\alpha \cos\gamma \sin(\omega t - \gamma) \tag{19}$$

After sufficient time, at steady state, $N - N_o^*$ varies as given by the last term of Eq. (19).

The MDSC measures the heat capacity by forming the appropriate averages over integral modulation cycles as ratio of the heat flow to temperature amplitudes. One finds, thus, that the apparent heat capacity $\Delta C_p^{\#}$ is $\varepsilon_h\, \alpha\, \cos\gamma$, the maximum amplitude of the phase-shifted heat flow $[\varepsilon_h \times (N - N_o^*)]$ divided by the temperature amplitude $A$. The polystyrene data of Fig. 3 can then be interpreted by fitting the experimental data. The phase lag $\gamma$ increases from zero at about 380 K to 90° at about 360 K. The (frequency dependent) glass transition temperature occurs at the point of half-devitrification, at a phase lag of 60°. Plotting the logarithm of $\tau_o$ as a function of $1/T$ one finds that the assumption of a temperature-independent $\tau$ is only an approximation. Different modulation frequencies lead to different activation energies. The values of $\log\tau_o$ at different amplitudes of modulation can, however, be extrapolated to zero amplitude to avoid the full solution of Eq. (12) with a temperature/time-dependent $\tau$.

For the derivation of the expression with modulation affecting the equilibrium number of holes $N^*$ and the relaxation time $\tau$, two normalized, dimensionless modulation amplitudes are introduced to describe the changes in $N$ and $\tau$ ($A_N = A\alpha/N_o$ and $A_\tau = A\varepsilon_j/(RT_o^2)$, respectively.)

Equation (6) becomes then:

$$N(t) = N_o\, e^{-t/\tau_o} + e^{-t/\tau_o} \int_{t_o}^{t} \frac{N_o^*(1 + A_N \sin\omega t')}{\tau_o(1 - A_\tau \sin\omega t')}\, e^{t/\tau_o}\, dt' \tag{20}$$

Because in integrating Eq. (20) one assumes steady state from Eq. (5), only the steady state solution can be utilized. It includes two components, one with the

phase angle $\gamma$, as given in Eqs (17) and (18), and one with the phase angle $2\beta$, given by:

$$2\beta = \arcsin \frac{2\omega}{\sqrt{(1/\tau_o)^2 + 4\omega^2}} \tag{21}$$

and:

$$2\beta = \arccos \frac{1/\tau_o}{\sqrt{(1/\tau_o)^2 + 4\omega^2}} \tag{22}$$

so that:

$$N - N_o^* = N_o^* \left[ \frac{A_N A_\tau}{2} + (A_N + A_\tau)\cos\gamma \sin(\omega t - \gamma) - \frac{A_N A_\tau}{2} \cos 2\beta \cos 2(\omega t - \beta) \right] \tag{23}$$

The level of $N$ about which modulation occurs is now higher than $N_o^*$ by $A_N A\tau/2$ and the second modulation term accelerates the relaxation during increasing $T$ and decelerates it on decreasing $T$. Figure 4 is a sample graph of such modulation. Again, the measured average over the integral modulation-cycles of the ratio of the heat flow to temperature amplitude is given by the equation $\Delta C_p^{\#} = (N_o^* \varepsilon_h / A)(A_N + A_\tau) \cos\gamma$. Note that the first term of Eq. (23) does not contribute to $\Delta C_p^{\#}$, and that last term has the frequency $2\omega$, double the

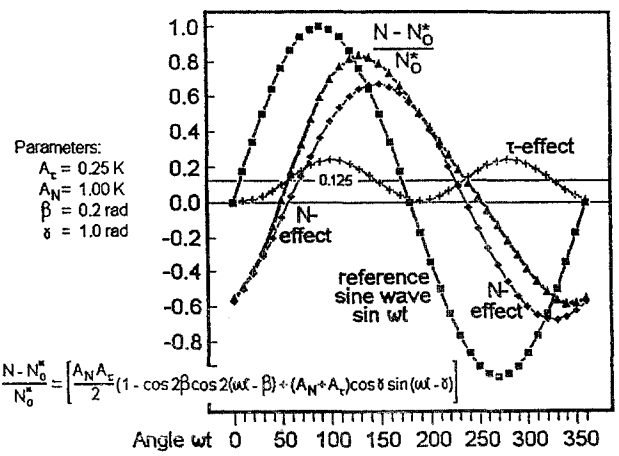


**Fig. 4** Modulation of the glass transition region. Filled squares represent the reference sine wave at the sample temperature position (phase-lag corrected due to heat conduction); Filled triangles give the modulation of the number of holes about the level 0.125 ($=A_N A_\tau/2$); The two thin lines indicate the two contributions to Eq. (23)

modulation frequency, and is, thus also not considered by MDSC. A full analysis of experimental data and a comparison with the earlier analysis of the irreversible enthalpy relaxation results [3] is given in part III of this discussion of MDSC in the glass transition region.

## Conclusions

The kinetics of the glass transition can be analyzed using MDSC if a number of conditions of steady state and negligible temperature gradient within the sample are obeyed. Based on the hole theory or irreversible thermodynamics a separation of the different contributions to the kinetics of the glass transition can be made (number of holes and relaxation time). A simplified analysis of experimental data by extrapolation to zero modulation amplitude is suggested. It is now possible to interpret the reversible and irreversible parts of the heat capacity in the glass transition region (apparent heat capacity and enthalpy relaxation, respectively). The equilibrium heat capacity is available through extra- polation of data outside of the glass transition for the solid and liquid.

* * *

The authors gratefully acknowledge constructive discussions with Dr. M. Reading, ICE Paints, Messrs. L. Thomas and B. S. Crowe of TA Instruments, Inc., R. Truttmann of Mettler-Toledo, and all attendees of the Third Lähnwitz Seminar, 1994. This work was financially supported by the Div. of Materials Res., NSF, Polymers Program, Grant # DMR 90-00520 and the Div. of Materials Sci., Office of Basic Energy Sciences, U. S. Department of Energy, under Contract DE-AC05-84OR21400 with Lockheed Martin Energy Systems. Support for instrumentation came from TA Instruments, Inc. and Mettler-Toledo, Inc. Research support was also given by ICI Paints, Exxon Res. and Eng. Co., Shell Development Co., and Toray Industries, Inc.



## References

1 M. Reading, Trends in Polymer Sci., 8 (1993) 248.
2 A. Hensel, J. Dobbertin, A. Boller, J. E. K. Schawe and C. Schick, J. Thermal Anal., 46 (1996) 935; J. E. K. Schawe, Thermochim. Acta, 261 (1995) 183.
3 B. Wunderlich, D. M. Bodily and M. H. Kaplan, J. Appl. Phys., 35 (1964) 95.
4 B. Wunderlich, Y. Jin and A. Boller, Thermochim. Acta, 238 (1994) 277.
5 Y. Jin, A. Boller and B. Wunderlich, Proc. 22nd NATAS Conf., 1993; and A. Boller, Y. Jin and B. Wunderlich, J. Thermal Anal., 42 (1994) 307.
6 B. Wunderlich, A. Boller, I. Okazaki and S. Kreitmeier, Thermochim. Acta, submitted, (1995).
7 A. Boller, C. Schick and B. Wunderlich, Proc. 23rd NATAS Conf., 1994. Full paper Thermochim. Acta, 266 (1995) 97.

8 A. Boller, I. Okazaki and B. Wunderlich, Proc. 24th NATAS Conf., S. A. Mikhail, editor, p. 136–141 (1995). Full paper by A. Boller, I. Okazaki and B. Wunderlich, in print Thermochim. Acta. (1966).
9 WWW (Internet), URL: http://funnelweb.utcc.utk.edu/~athas.
10 B. Wunderlich, 'Thermal Analysis,' Academic Press, Boston 1990.
11 B. G. Sumpter, D. W. Noid and B. Wunderlich, Adv. Polymer Sci., 116 (1994) 27.
12 B. Wunderlich and J. Grebowicz, Adv. Polymer Sci., 60/61 (1984) 1.
13 B. Wunderlich, J. Phys. Chem., 64 (1960) 1052.
14 G. Tammann,'Der Glaszustand.' Leopold Voss, Leipzig 1933.
15 R. G. Seyler, editor, 'Assignment of the Glass Transition', ASTM Symposium, March 4–5, 1993, Atlanta, GA. STP 1249, Am. Soc. Testing of Materials, Philadelphia, 1994.
16 B. Wunderlich, 'The Nature of the Glass Transition and its Determination by Thermal Analysis,' Ref. 15 p. 17–31.
17 B. Wunderlich, Colloid and Polymer Sci., 96 (1994) 22.
18 H. Eyring, Chem. Phys., 4 (1936) 238; J. Frenkel, 'Kinetic Theory of Liquids.' Clarendon Press, Oxford, England 1946.
19 Contact the authors for summaries of the data bank, or see Ref. [9] and B. Wunderlich, Shin Netsu Sokuteino Shinpo, 1 (1990) 71, or Pure and Applied Chem., 67 (1995) 1919.
20 N. Hirai and H. Eyring, J. Appl. Phys., 29 (1958) 810; J. Polymer Sci., 37 (1959) 51.
21 M. V. Vol'kenstein and O. Ptitsyn, Zh. Tekhn. Fiz., 26 (1956) 2204.